NASA Contractor Report 3835

Dynamic Model of the Earth's Upper Atmosphere

Jack W. Slowey

CONTRACT NAS8-34947
SEPTEMBER 1984

NASA

NASA Contractor Report 3835

Dynamic Model of the Earth's Upper Atmosphere

Jack W. Slowey
Smithsonian Institution
Cambridge, Massachusetts

Prepared for
George C. Marshall Space Flight Center
under Contract NAS8-34947

National Aeronautics
and Space Administration

Scientific and Technical
Information Branch

1984

CONTENTS

DYNAMIC MODEL OF TEE EARTH'S UPPER ATMOSPHERE

1.0 INTRODUCTION

Altbough high resolution data from satellite-borne mass spectrometers, accelerometers and other instruments have contributed greatly to our understanding of the phy'sics of the neutral upper atmosphere, the older atmospheric models, based entirely on satellite drag analysis, remain viable in most applications to orbital mechanics. The more recent models, such as MSIS and J77, represent composition and changes in composition more accurately than do the models based on drag. For the most part, however, they are not significantly better in their representation of the total density. This, combined with the greater complexity and computing costs of the more recent models, argues strongly for continued use of the older models in those situations where the representation of total density and variations in total density are the only criteria of model performance.

The drag-based models are deficient in the way they represent the large variations in total density that are associated with geomagnetic disturbances, however. These variations are represented in the models as being uniform over the globe, while the more recent high resolution data have shown them to have very significant global structure, mainly in relation to geomagnetic latitude. This is a matter of concern in a number of currently important applications where it is necessary to accurately predict the density and its variations on a local basis. For this reason, we undertook the task of modifying the J70 atmospheric model used at MSFC to include a high resolution model of the geomagnetic variation in the thermosphere and exosphere.

The model of the geomagnetic variation that we included is an improved version of the one that we developed from analysis of the ESRO 4 mass spectrometer data and that was incorporated in Jacchia's 1977 comprehensive model. It is described in detail in Appendix A. It includes the variation with geomagnetic local time as well as with geomagnetic latitude and also includes the effects due to disturbance of the temperature profiles in the region of energy deposition. The implementation of the model in the MSFC program is described in the next section.

2.0 MODEL IMPLEMENTATION

The high resolution model of the geomagnetic variation described in Appendix A was implemented in computer software by modification of the J70-3 program used at MSFC. A copy of the FORTRAN source file for this program was supplied to us in card form. The source file for the modified program, which we designated J70-3X, has, in turn, been shipped to MSFC in card form together with a compiler listing of the program and samples of the output that it produces.

Modification of the program included revision of the main program and the TINF and JAC subroutines and addition of the subroutines GANG, CONGI and AVER. The labeled common block MAGMOD was introduced to aid in communication between the different program units. The hyperbolic tangent was also introduced in several locations as an assumed library function.

The modified program provides for optional calculation of the geomagnetic variation according to either the 1970 Jacchia model, as in the original program, or the 1971 Jacchia model rather than the high resolution model. In addition, the high resolution model may be specified in either of two diurnally-averaged forms rather than in unaveraged form.

2.1 Modes of Operation

The modified program operates in one of five possible modes relative to the calculation of the effects of the geomagnetic variation. The particular mode is specified by a parameter that was added at the end of the "case" list that is a part of the control input to the program. The addition of this parameter, MODE, was the only change made to the program input. Calculation of the geomagnetic variation in the different modes is described briefly in the following subsections.

2.1.1 571 Geomagnetic Model, MODE = -1

In this mode, the geomagnetic variation is calculated according to equations 18 and 20 of Jacchia's 1971 model atmosphere. Equation 18 provides only for an increase in exospheric temperature and applies to heights above 350 km. It is identical to the equation given for the geomagnetic variation in Jacchia's 1970 model and was derived in one of our

earlier studies of satellite drag. It does not give good results below about 200 km because the variation of density with exospheric temperature in the static models is too small to adequately represent the geomagnetic variation at those heights. Equation 20 includes a direct increase in density in addition to an increase in exospheric temperature and gives better results at low heights, We employed the same interpolation scheme used in the implementation of the 1971 model included in the 1972 CIRA to make a smooth transition between the two equations in the vicinity of 350 km. This mode was included in order to provide a more suitable standard of comparison for the high resolution model at low heights,

2.1.2 J70 Geomagnetic Model, MODE = 0

In this mode, the geomagnetic variation is calculated according to the equations given with Jacchia's 1970 model atmosphere. Results in this mode are identical to those obtained with the original version of the program. Note that the program provides for calculation using either equation 21 or equation 22 of the 1970 model, depending on whether the K_p geomagnetic index or the equivalent a_p index is specified in the input, At present, however, the relevant indicator is set internally in the program so that the value in the input is always assumed to be the a_p index.*

2.1.3 Local-Time-Averaged Model, MODE = 1

In this mode, the high resolution model of the geomagnetic variation is used, but an average is taken over local time. The results represent daily averages for points above a fixed location on the surface of the earth and will depend on the geomagnetic latitude that corresponds to the geocentric latitude and longitude specified in the input.+ This mode was

---

* This is true regardless of the operating mode that is specified. None of the other modes provide for direct calculation using the a_p index, however. Instead, the a_p index, when indicated, is converted to the equivalent K_p index by a call to the subroutine CONGI prior to entry in the programmed equations.

+ It would have been appropriate to have the program print the geomag-

provided mainly for diagnostic and developmental purposes.

2.1.4 Longitude-Averaged Model, MODE = 2

In this mode, the high resolution model of the geomagnetic variation is used, but an average is taken over longitude. The apparent solar time, as determined by the geocentric longitude and the GMT given in the input, is kept constant. In this case, the results represent daily averages as would be seen by an orbiting object at the point in its orbit corresponding to the geocentric latitude and longitude and the GMT specified in the input. This mode would, therefore, be appropriate in orbital integration or a comparison with drag measurements where the time step is a day or more. Note that, while considerable smoothing will occur in high latitudes, a strong local time dependence will remain in middle and low latitudes in addition to the dependence on latitude. For this reason, the program prints the apparent solar time in the output along with the specified latitude and longitude. Also note that both diurnally-averaged modes (MODE = 1 or 2) are somewhat more expensive to run than the non-averaged mode (MODE = 3), since the averages are obtained numerically* by summing values taken at 10-degree intervals around the globe. Although no detailed comparisons were made, this is not expected to be very significant compared to the total cost of running the program, however.

2.1.5 Complete High-Resolution Model, MODE = 3

In this mode, the geomagnetic variation is Calculated according to the improved high-resolution model developed from mass spectrometer observations. Most of the details of this model, including the values of the constants used, are given in Appendix A. In this mode there is no averaging and the results are directly dependent on both the geomagnetic latitude and the geomagnetic local time, both of which are calculated from the nor-

---

netic latitude in the output along with the specified geocentric latitude and longitude in this mode. This, however, was overlooked in the programming process.

* The averaging is done in subroutine AVER for either diurnally-averaged mode.

mal input to the program. The calculation is that for a centered dipole.. The geomagnetic latitude and geomagnetic local time are both printed with the specified geocentric latitude and longitude in the output. As in all of the modes involving the high resolution model, the temperature profiles are assumed to be perturbed according to equation 32 of Jacchia's 1977 atmospheric model,

$$\Delta_G T(z) = \Delta_G T_\infty \tanh[0.006(z - 90.0)],$$

where z is in km. This equation is incorporated directly in the integration of the diffusion equation in subroutine JAC. It permits the effects of geomagnetic disturbance to be accurately represented even at very low thermospheric heights.

2.2 Computation of Geomagnetic Coordinates

The high resolution model is a function of both the geomagnetic latitude and the geomagnetic local time. These angles are computed from the geocentric latitude and longitude and the solar declination and hour angle in subroutine GANG, assuming the earth's magnetic field to be represented by a centered dipole.

The geomagnetic latitude, ϕ_G, is easily computed[+] from

$$\sin\phi_G = \sin\phi \sin\phi_p + \cos\phi \cos\phi_p \cos(\lambda - \lambda_p), \qquad (1)$$

where ϕ and λ are the geocentric latitude and east longitude, respectively, of the point in question and ϕ_p and λ_p are the geocentric latitude and east longitude, respectively, of the boreal geomagnetic pole. We assumed ϕ_p =

---

* The (adiabatically) invariant geomagnetic coordinates seem to correlate best with small details of the geomagnetic variation, but the differences between the two coordinate systems are small and the dipole coordinates are entirely adequate for our purposes here.

+ The coordinate conversion described in this section is illustrated in "Coordinate systems based on the geomagnetic field" in the International Dictionary of Geophysics, Vol. 1, pp. 616-617. The equations given in that article are not fully developed for machine computation as are those given here, however.

79.0 degrees and λ_p = 291.0 degrees.

To compute the geomagnetic local time, we first compute the "geomagnetic longitude", λ_G, which is the angle. measured counterclockwise at the geomagnetic pole, between the geographical meridian extending southward from the geomagnetic pole and the great circle through the geomagnetic pole and the point in question. We have

$$\begin{aligned} \sin k &= \frac{\cos\phi \sin(\lambda - \lambda_p)}{\cos\phi_G} \\ \cos\lambda_G &= \frac{\sin\phi_p \sin\phi_G - \sin 4}{\cos\phi_p \cos\phi_G} . \end{aligned} \tag{2}$$

These equations become Undefined in the case where $\cos\phi_G = 0$ (i.e., where the point in question is at one of the geomagnetic poles). In that case, we set $\lambda_G = 0$.

Next, we compute $\cos\beta$ and $\sin\beta$, where β is the angle between the geomagnetic pole and the direction of the anti-sun. We have

$$\begin{aligned} \cos\beta &= -\sin\phi_p \sin\delta_s + \cos\phi_p \cos\delta_s \cos(t + \lambda_p - \lambda) \\ \sin\beta &= (1 - \cos^2\beta)^{\frac{1}{2}} , \end{aligned} \tag{3}$$

where δ_s is the solar declination angle and t is the apparent solar time (= solar hour angle + π radians) at the point in question. Taking $\sin\beta$ to be always positive merely implies that β lies between 0 and π radians, as it should.

We then compute the "geomagnetic time" of the geographical meridian that passes through the geomagnetic pole. This we define to be the angle, measured counterclockwise at the pole. between the great circle through the pole and the anti-sun position and the southward extension of the meridian that passes through the pole. Calling this angle Δt_G, we have

$$\begin{aligned} \sin\Delta t_G &= \frac{\cos\delta_s \sin(t + \lambda_p - \lambda)}{\sin\beta} \\ \cos\Delta t_G &= \frac{\sin\delta_s + \cos\beta \sin\phi_p}{\sin\beta \cos\phi_p} . \end{aligned} \tag{4}$$

Since neither $\sin\beta$ or $\cos\phi_p$ can be equal to zero, there is no problem with these equations becoming undefined. We can then compute the geomagnetic local time, t_G, which is given by

$$t_G = \lambda_G + \Delta t_G. \tag{5}$$

A good approximation to the geomagnetic local time is given by

$$t_G \approx t + \lambda_p + \lambda_G - \lambda, \tag{6}$$

which eliminates evaluation of equation 3 and the determination of Δt_G from equation 4. The savings that could be gained by using the approximation were not thought to be significant in terms of the total cost of running the program, however, and exact computation of the geomagnetic local time, utilizing equations 2 through 5, was implemented.

2.3 Equatorial Wave Modification

As given by equation A-12 of Appendix A, the "equatorial wave" component of the high resolution model consists of a proportional increase in density that is independent of height. That this component of the geomagnetic variation should be independent of height in the lower thermosphere is not physically realistic and represents a flaw in the formulation of the model. To correct this flaw in the implementation of the model, we developed the following expression to replace the original equation for the equatorial wave:

$$\Delta_e \log n_i = \Delta_e \log \rho = 6.55 \times 10^{-4} \tanh[0.006(z - 100.0)] A \cos^2 \theta, \tag{7}$$

where ρ is the total density and A is the polar increase in exospheric temperature given by equation A-3 of Appendix A. With this modification, the high resolution model gives density variations at low heights in the equatorial region that are in good agreement with those reported by Marcos et al* from lor-altitude accelerometer measurements made in a number of satellite experiments at heights down to about 140 km.

---

* Marcos, F.A., D.F. Gillette, and E.C. Robinson, 1982: A Global Thermospheric Density Model Based on Satellite Accelerometer Data, AFGL-TR-82-0025.

24 Weighted-Mean Geomagnetic Index

The geomagnetic index is specified as one of the input parameters to the J70-3 atmospheric model program. Thus, we were not able to implement calculation of a weighted-mean value of the index as specified by equation A-5 of Appendix A. If the program is to be used to simulate actual variations in the atmosphere, we strongly recommend that this be done, however, and that the weighted-mean index be used as input to the program.* We would be happy to assist MSPC in whatever way is required to achieve this end.

Since we first introduced the idea of using a weighted-mean index in our model of the geomagnetic variation, we have discovered confirmation of it in the work of others in the field. Nisbet et al[+] combined this idea with use of an auroral electrojet index in a study of atomic oxygen variations observed by the OSS mass spectrometer on the *AE-C* satellite during two geomagnetic storm periods. They obtained significantly better representations of the observed variations than could be obtained using individual values of the 3-hour a_p index. Of course, this may have been due in part to the superiority of the electrojet index as an indicator of disturbance in the atmosphere. It is worth noting, however, that the time constants (≈24 hours) that were found to give the best results for the recovery phases of the storms are entirely consistent with the one that we arrived at quite independently from our examination of the ESRO 4 and AE-C mass spectrometer data. More recently, Hedin[‡] has included an index based on a similar "summation formula" for use with the model of the geomagnetic variation in his latest version of the MSIS thermospheric model. He gives an example in which this index is utilized that shows how the "rise and

---

* The concept of a weighted-mean of the geomagnetic index as an index of atmospheric disturbance is not, of course, limited to the high resolution model. It applies to any model of the geomagnetic variation.

[+] Nisbet, J.S., C. Stehle, and E. Bleuler, 1983: Initial tests of an index based on AL values for modeling magnetic storm related perturbations of the thermosphere, J. Geophys. Res., 88, pp. 2175-2180.

[‡] Hedin, A.E., 1983: A revised thermospheric model based on mass spectrometer and incoherent scatter data: MSIS-83, J. Geophys. Res., 88, pp. 10170-10188.

fall of the density predicted using the summed three hour indices is much more representative of the data than either the prediction based on the daily index or the variation of the 3-hour index itself." He uses separate time constants for the exospheric temperature and each of the various constituents and finds the values of these to vary between 6.9 hours and 13.0 hours. His value for atomic oxygen, rhioh is most important as far as total density is concerned at most heights, is 11.4 hours. Thus, while he confirms the applicability of the concept, his estimate of the time constant is somewhat smaller than was indicated by our work and that of Nisbet et al. We hope to be able to pursue the question of the best value of the time constant further, utilizing a larger portion of the mass spectrometer data that we have.

APPENDIX A

A NEW MODEL OF THE GEOMAGNETIC VARIATION IN THE UPPER ATMOSPHERE*

A.1 INTRODUCTION

Large variations in the density of the thermosphere and exosphere in association with geomagnetic disturbances were first detected by Jacchia (1959, 1961) in the drag on artificial satellites. Densities obtained from the analysis of drag were then used extensively to study and model this geomagnetic variation in the upper atmosphere. Model development based on drag analysis culminated with the model derived by Jacchia *et al* (1967) that was subsequently incorporated, with only slight modification, in the 1972 CIRA reference atmosphere and other general models of the upper atmosphere derived from drag analysis.

The models of the geomagnetic variation based on drag analysis were extremely simple in form and usually represented the variation as being uniform over the globe. As it turns out, the geomagnetic variation is extremely complex in form but, while this was certainly suspected, the drag data revealed few details because of their poor resolution. It was not until data from *in situ* accelerometer and mass spectrometer experiments became available that the geomagnetic variation could be modeled in any detail. The process is still far from being complete, however.

There are, at present, two models based on high-resolution data in use. One of these is that of Jacchia *et al* (1976, 1977) that is incorporated in Jacchia's most recent general model of the thermosphere and exosphere (1977). The other is that of Hedin *et al* that is incorporated in the MSIS model (1977a, 1977b, 1979). Here, we will describe initial efforts directed toward extending and improving the model of Jacchia *et al*. In this, we have four main aims. These are:

1) To incorporate the variation with local magnetic time. As it is now, the model includes only the mean variation with latitude. The local time variation is extremely complex, but the main features are quite significant and can be included without too much difficulty.

---

* This is a reproduction of a paper originally presented at the Ninth Conference on Aerospace and Aeronautical Meteorology in Omaha in June, 1983, and later published as USAF Report AFGL-TR-83-0253.

2) To allow the form of the variation to vary with the level of disturbance. Slowey (1981) has shown the latitudinal form of the variation to broaden in high latitudes with increasing levels of disturbance. This effect appears to be related to a shift in the location of some of the heat input. Yeng (1982) has reported that the polar cusp region shifts significantly toward lower latitudes for larger disturbances,

3) To allow for the prior heat input in establishing an index for the level of disturbance. The K_p geomagnetic index admittedly leaves much to be desired as an indicator of disturbance in the atmosphere. It is increasingly clear, however, that there is much to be gained by taking account of the persistence of the effects of disturbance. Theoretical calculations such as those by Faller-Rowel1 and Rees (1981) and the semiempirical models of Hedin et al (1981) indicate that the disturbance history over the preceding 5 days is probably significant.

4) To correct what is now seen as a rather serious flaw in the original model in not permitting an increase in exospheric temperature at the equator. The effect at the equator was modeled entirely in terms of an "equatorial wave" of density that was assumed to originate in high latitudes and progress towards the equator. While it is clear from the mass spectrometer data that such a wave is a significant component of the low latitude response, it is now equally clear that a thermal component also exists in low latitudes. Separating the two components in data from a single height or from a limited range of height, which was all that was available to us until recently, is extremely difficult, however, and a final determination of the relative importance and extent of the equatorial wave will depend on future analysis of data from lower heights.

A2 NATURE OF TEE VARIATION

In figure A-1 we show a plot of molecular nitrogen density measured during a portion of one orbit of the Atmosphere Explorer-C satellite by the OSS mass-spectrometer. The data were collected during a period of relatively high geomagnetic activity (1.5 hours earlier, K_p was 6+) and when the satellite was in a nearly circular orbit. Since the height varied so little, in was safe to reduce them to a single height for purposes of analysis and that is the way they are shown here. The abscissa is the time in minutes, starting from an arbitrary zero point. The scale of the ordinate of the N_2 number density is not shown, but it represents the change in the logarithm of the number density. The maximum density here corresponds to a change of 0.5 in $\log_e n(N_2)$, an increase by a factor of more than 3 in number density, relative to the density at the origin of the plot. The smooth curve at the top of the figure is the (adiabatic invariant) geomagnetic latitude plotted on the scale at the left of the figure.

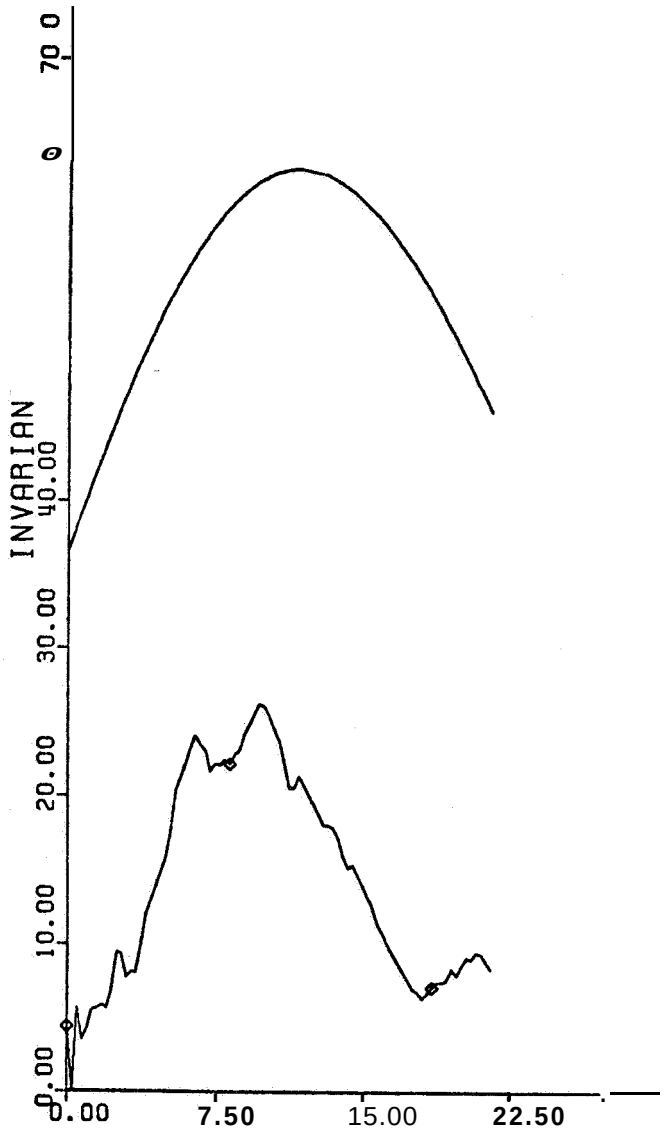

Figure A-1. Logarithm of N, density at a height of 250 km as measured by the OSS mass spectrometer on AE-C during a portion of orbit 4919. The abscissa is the time in minutes from an arbitrary zero point and the ordinate is not given (see text). The smooth curve is the invariant geomagnetic latitude with ordinate scale on the left.

The strong dependence of the geomagnetic variation on geomagnetic latitude is well established and we can see it in orbit after orbit of the AE-C and other satellite-borne mass Spectrometer data, not only in N, but in all constituents. Not all constituents behave the nay N_2 does, however, and this is another important aspect of the geomagnetic variation. The behavior of the lighter constituents, such as He, is just the opposite of that of N_2: their number densities decrease where those of N_2 increase. And the density of atomic oxygen, which is of primary importance as far as total density is concerned throughout most of the thermosphere, may either

increase, decrease or remain unchanged. In addition to a purely thermal effect, there is another factor involved in which the molecular mass is very important. We shall represent this factor in terms of a variation in the height of the homopause.

The variation is also clearly not just dependent on the geomagnetic latitude. There are two distinct maxima in the data of figure A-1 that represent separate regions of enhancement in the vicinity of the auroral oval. As the figure demonstrates, there is also an appreciable over-all asymmetry with respect to geomagnetic latitude,

A.3 FORM OF THE MODEL

The model of Jacchia et al represents the density and composition changes that occur in association with a geomagnetic disturbance by a local increase in exospheric temperature and a proportional increase in the height of the homopause. The increase in the height of the homopause is a convenient device by which to represent an effect (the inverse variation of the lighter constituents) that may actually be due more to wind-induced vertical diffusion. Superimposed on these two effects is the "equatorial wave" referred to in the introduction, in which the number densities of all constituents increase in the same proportion and that is centered on the equator. We will adopt the same representation here and model the change in the logarithm of the number density of the species i as the sum of three components:

$$\Delta_G \log n_i = \Delta_T \log n_i + \Delta_H \log n_i + \Delta_e \log n_i \qquad \text{(A-1)}$$

where $\Delta_T \log n_i$ is the thermal component, $\Delta_H \log n_i$ is the component due to the change in the height of the homopause and $\Delta \log n_i$ is the component due to the equatorial wave. The thermal component $\Delta_T \log n_i$ is to be evaluated from an atmospheric model assuming an increase in exospheric temperature $\Delta_G T_\infty$ given by

$$\Delta_G T_\infty = A F(\phi, \lambda) \qquad \text{(A-2)}$$

where A is the amplitude given by

$$A = 57.5 K_p' [1 + 0.027 \exp(0.4 K_p')] \ , \qquad \text{(A-3)}$$

as in the earlier model, and $F(\phi,\lambda)$ is given by

$$\begin{aligned} F(\phi,\lambda) = {} & a_{01} + a_{02} \sin^n \phi + \\ & \cos^2 \phi (a_{11} \sin\lambda + a_{12} \cos\lambda) + \\ & \sin 2\phi (a_{21} \sin\lambda + a_{22} \cos\lambda) + \\ & \sin^4 \phi \sin 2\phi (a_{31} \sin\lambda + a_{32} \cos\lambda) \ , \end{aligned} \qquad \text{(A-4)}$$

where ϕ and λ are the geomagnetic latitude and local magnetic time, respectively. To take the effects of persistence into account, we assume K_p' in equation A-3 to be the weighted mean of the lagged 3-hourly K_p geomagnetic index taken over the 41 values in the preceding 5-day interval as follows:

$$K_p'(t) = \frac{\sum_{t_i=t-\tau-5}^{t-\tau} K_p(t_i) e^{-c(t-t_i-\tau)}}{\sum_{ti=t-\tau-5}^{t-\tau} e^{-c(t-t_i-\tau)}} \qquad \text{(A-5)}$$

where t is the time in days, c = 1.0 d^{-1} and τ is the time lag given by

$$\tau = 0.05 + 0.1 \cos^2 \phi \ \text{(day)} \qquad \text{(A-6)}$$

In equation A-4, the first two terms represent the mean latitudinal variation of the increase in exospheric temperature. The remaining three terms represent the variation of the temperature increase with local magnetic time (LMT) in low, middle and high latitudes, respectively. To introduce a variation in the mean shape of the latitudinal variation with the level of disturbance, we take n in equation A-4 as

$$n = 5.0 - K_p'/3.0 \qquad \text{(A-7)}$$

A preliminary determination of the remaining parameters in equation A-4 was made by a least squares fit to values of the exospheric temperature increase inferred from N_2 measurements made by the ESRO4 mass spectrometer. Exospheric temperatures were obtained from N_2 densities by inverse interpolation in an atmospheric model. The temperature increase was taken to be the difference between the exospheric temperature corresponding to the observed N_2 density and that corresponding to the density computed for quiet conditions from the ESRO4 "quiet time" model of von Zahn *et al* (1977). The resulting coefficients are

$$\begin{aligned} a_{01} &= .1425E{+}00 & a_{02} &= .8137E{+}00 \\ a_{11} &= .1184E{+}00 & a_{12} &= -.3604E{-}01 \\ a_{21} &= -.7354E{-}01 & a_{22} &= .1038E{+}00 \\ a_{31} &= .3706E{+}00 & a_{32} &= -.1441E{+}00 \end{aligned} \qquad \text{(A-8)}$$

The isotherms of the relative temperature increase as given by equation A-4 in the case where $K_p' = 3$ ($n = 4$) are plotted over the globe in geomagnetic coordinates in figure A-2. As can be seen, there is a considerable asymmetry with respect to the pole. The maximum is between 6^h and 9^h at a latitude of about 80 degrees. This probably reflects both Joule heating by the westward auroral electrojet and particle precipitation in the cusp region. The extent of the asymmetry can perhaps be better seen in figure A-3, where the profiles for 6^h and 18^h LMT - near the extremes - are plotted together with the mean latitudinal profile. Of course, the difference in high latitudes as seen by an orbiting object would tend to be smoothed out over intervals on the order of a day because of the earth's

rotation. This would not be the case in low latitudes, however, and it is interesting to note that, even with the poor resolution of satellite drag, Roemer (1971) was able to detect this asymmetry in densities deduced from drag.

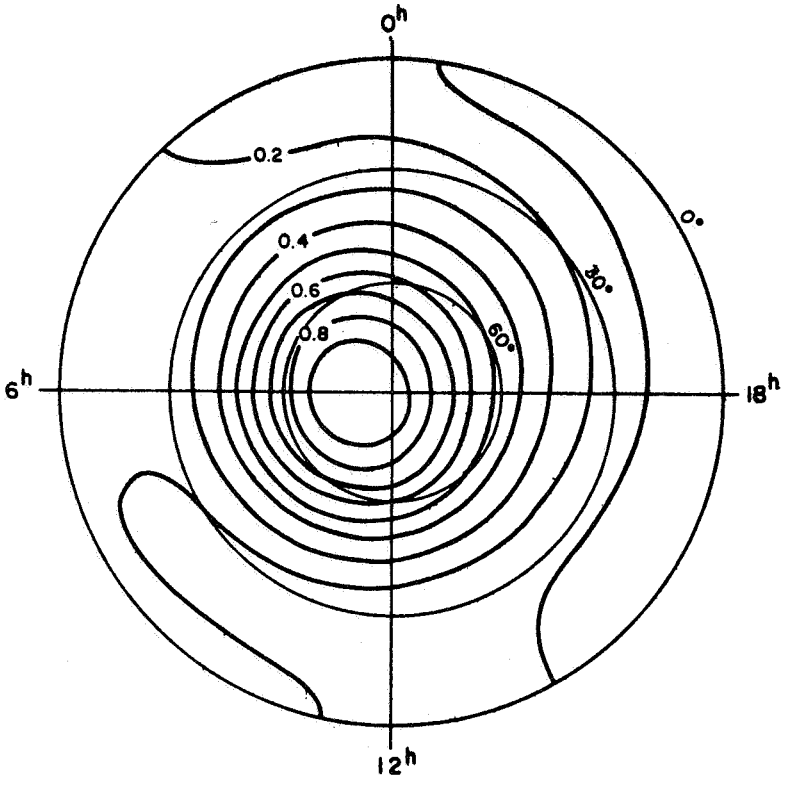

Figure A-2. Global isotherms of the relative temperature increase due to geomagnetic disturbance as given by equation A-4 for $K_p' = 3$. The coordinates are geomagnetic latitude and magnetic local time.

We should point out that a geomagnetic disturbance will alter the atmospheric temperature profiles, so that the procedure we have outlined of entering exospheric temperatures in a static model to determine the effects on the number densities is not strictly valid. There will be a height dependence that we have not accounted for that becomes an important consideration at lower heights. In this connection. we have developed disturbed temperature profiles that give good results in representing observed density variations at heights as low as 150 km. We have also developed expressions to represent the effects of these disturbed profiles on the number densities analytically. These expressions are rather involved. so we will not repeat them here, but they represent an integral part of the thermal component of the geomagnetic variation as we would model it.

Concerning the other two components of the geomagnetic variation, we would include them in the form given recently by Slowey (1983). Specifically, we would compute the component due to the change in the height of

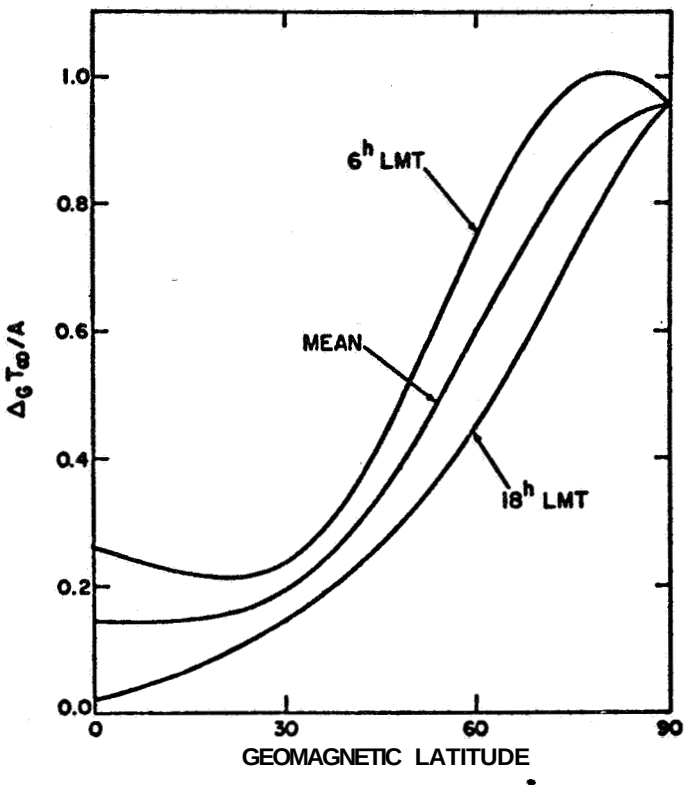

Figure A–3. Latitude profiles of the relative temperature increase for $K_p' = 3$ as given by equation A–4 for 6^h and 18^h LMT. The profile of the mean latitudinal variation is also shown.

the homopause from

$$\Delta_H \log n_i = \alpha_i \Delta z_H, \tag{A–9}$$

where Δz_H (meters) is to be computed from

$$\Delta z_H = 22.0\, \Delta_G T_\infty \ , \tag{A-10}$$

where $\Delta_G T_\infty$ is given by equation A-2. and the ai's are:

$$\begin{aligned} \alpha(Ar) &= +3.07 \times 10^{-5} \quad \text{(mks)} \\ \alpha(O_2) &= +1.03 \times 10^{-5} \quad \text{(mks)} \\ \alpha(N_2) &= 0.0 \\ \alpha(O) &= -5.75 \times 10^{-5} \quad \text{(mks)} \\ \alpha(He) &= -6.30 \times 10^{-5} \quad \text{(mks)} \ . \end{aligned} \tag{A-11}$$

The component due to the equatorial wave would be computed from

$$\Delta_e \log n_i = \Delta_e \log \rho = 5.2 \times 10^{-4} A \cos^2 \phi \tag{A-12}$$

where p is the total density and A is given by equation A-3. As was mentioned in the introduction, some work remains to be done to better separate this component from the thermal component in low latitudes. Suitable data are available from both mass spectrometer and accelerometer experiments.

REFERENCES

Fuller-Rowell, T. J., and D. Rees, 1981: A three-dimensional, time-dependent simulation of the global dynamical response of the thermosphere to a geomagnetic substorm. J. Atmos. Ter. Phys., Vol. 43, pp. 701-721.

Hedin, A. E., J. E. Salah, J. V. Evans, C. A. Reber, G. P. Newton, N. W. Spencer, D. C. Kayser, D. Alcayd, P. Bauer, L. Cogger, and J. P. McClure, 1977a: A global thermospheric model based on mass spectrometer and incoherent scatter data; MSIS 1, N_2 density and temperature. J. Geophys. Res., Vol. 82, pp. 2139-2147.

Hedin, A. E., C. H. Reber, G. P. Newton, N. W. Spencer, H. C. Brinton, and H. G. Mayr, 1977b: A global thermospheric model based on mass spectrometer and incoherent scatter data; MSIS 2, Composition. J. Geophys. Res., Vol. 82, pp. 2148-2156.

Hedin, A. E., C. A. Reber, N. W. Spencer, H. C. Brinton, and D. C. Kayser, 1979: Global model of longitude/UT variations in thermospheric composition and temperature based on mass spectrometer data. J. Geophys. Res., Vol. 84, pp. 1-9.

Hedin, A. E., H. W. Spencer, H. G. Mayr, and H. S. Porter, 1981: Semiempirical modeling of thermospheric magnetic storms. J. Geophys. Res., Vol. 86, pp. 3515-3518.

Jacchia, L. G., 1959: Corpuscular radiation and the acceleration of artificial satellites. Nature, Vol. 183, pp. 1662.

---, 1961: Satellite drag during the events of November 1960. Space Research II, North-Holland Publ. Co., Amsterdam, pp. 747-750.

----, 1977: Thermospheric temperature, density, and composition: new models. Smithsonian Astrophys. Obs. Spec. Rep. No. 375, 106 pp.

Jacchia, L. G., J. Slowey, and F. Verniani, 1967: Geomagnetic perturbations and upper atmospheric heating. J. Geophys. Res., Vol. 72, pp. 1423-1434.

Jacchia, L. G., J. W. Slowey, and U. von Zahn, 1976: Latitudinal changes in composition in the disturbed thermosphere from ESRO 4 measurements. J. Geophys. Res., Vol. 81, pp. 36-42.

---- ---- and ----, 1977: Temperature, density, and composition in the disturbed thermosphere from ESRO 4 gas analyzer measurements: a global model. J. Geophys. Res., Vol. 82, pp. 684-688.

Meng, C.-I., 1982: Latitudinal variation of the polar cusp during a magnetic storm. Geophys. Res. Lett., Vol. 9, pp. 60-63.

Roemer, M., 1971: Geomagnetic activity effect on atmospheric density in the 250 to 800 km altitude region. Space Research XI, Akademie-Verlag, Berlin, pp. 965-974.

Slowey, J. W., 1981: Models of the geomagnetic effect in the earth's thermosphere. Adv. Space Res., Vol. 1, pp. 213-219.

----, 1983: The Geomagnetic Variation in the Upper Atmosphere. Adv. Space Res., Vol. 3, pp. 67-73.

von Zahn, U., W. Köhnlein, K. H. Fricke, U. Laux, H. Trinks, and H. Volland, 1977: ESRO 4 model of global thermospheric composition and temperatures during times of low solar activity. Geophys. Res. Lett., Vol. 4, pp. 33-36.

1. REPORT NO.	2. GOVERNMENT ACCESSION NO.	3. RECIPIENT'S CATALOG NO.
NASA CR-3835		

4. TITLE AND SUBTITLE	5. REPORT DATE
Dynamic Model of the Earth's Upper Atmosphere	September *1984*
	6. PERFORMING ORGANIZATION CODE
7. AUTHOR(S)	8. PERFORMING ORGANIZATION REPORT #
Jack W. Slowey	
9. PERFORMING ORGANIZATION NAME AND ADDRESS	10. WORK UNIT NO.
Smithsonian Institution Astrophysical Observatory Cambridge, Massachusetts *02138*	M-462
	11. CONTRACT OR GRANT NO.
	NAS8-34947
	13. TYPE OF REPORT & PERIOD COVERED
12. SPONSORING AGENCY NAME AND ADDRESS	Final report for the period Aug. 27, 1982 - Feb. 26, 1984 Contractor Report
National Aeronautics and Space Administration Washington, DC *20546*	14. SPONSORING AGENCY CODE

15. SUPPLEMENTARY NOTES

Marshall Space Flight Center, Systems Dynamics Laboratory
Technical Monitor: Dr. Robert E. Smith

16. ABSTRACT

This report presents an initial modification to the MSFC/J70 Thermospheric Model, in which the variations due to sudden geomagnetic disturbances upon the aarth's upper atmospheric density structure has been modeled. This dynamic model of the geomagnetic variation included is an improved version of one which SAO developed from the analysis of the ESRO *4* mass spectrometer data that was incorporated in the Jacchia *1977* model. It includes the variation with geomagnetic local time as well as with geomagnetic latitude, and also includes the effects due to disturbance of the temperature profiles in the region of energy deposition.

17. KEY WORDS	18. DISTRIBUTION STATEMENT
Geomagnetic Variation Thermosphere Atmospheric Density Atmospheric Constituents Upper Atmosphere Atmospheric Model	Unclassified - Unlimited Subject Category *47*

19. SECURITY CLASSIF. (of this report)	20. SECURITY CLASSIF. (of this page)	21. NO. OF PAGES	22. PRICE
Unclassified	Unclassified	21	A02

For sale by National Technical Information Service, Springfield. Virginia 22161 NASA-Langley, 1984